Enhancement of Proton Transport in Pyroelectric Crystal Acceleration Using a Novel Negative Target Configuration

Shun INOUE[1)], Toru TAKAHASHI[1)], Siyu ZHANG[1)], Kanato YURI[2)], Yuxuan XU[1)], Zhichao ZUO[1)], Ryosuke KOIZUMI[3)], Yuto SUZUKI[3)], Suguru NOZAWA[3)], Shota MORISHITA[3)], Toshiki TAKAHASHI[1)]*, Masahiko SATO[4)]

[1)] *Graduate School of Science and Technology, Gunma University, 1-5-1 Tenjin-cho, Kiryu, Gunma 376-8515, Japan*
[2)] *Interfaculty Initiative in Regulatory Science of Biomedical Science and Engineering, Gunma University, 1-5-1 Tenjin-cho, Kiryu, Gunma 376-8515, Japan*
[3)] *School of Science and Technology, Gunma University, 1-5-1 Tenjin-cho, Kiryu, Gunma 376-8515, Japan*
[4)] *National Institute for Fusion Science, National Institutes of Natural Sciences, 322-6 Oroshi-cho, Toki, Gifu 509-5292, Japan*

(Received 11 June 2026 / Accepted 24 June 2026)

In this study, numerical simulations were performed to compare a conventional positive Disk Electrode configuration with a newly proposed Negative Target configuration for proton acceleration. Electrostatic potentials were calculated by solving Laplace's equation, and proton generation was modeled through hydrogen ionization reactions coupled with charged-particle trajectory calculations. The results showed that no protons reached the target in the conventional Disk Electrode configuration. In contrast, the Negative Target configuration produced substantial proton impacts, with the maximum proton count obtained at crystal temperature changes of 2.5–5 K. Furthermore, the introduction of a positively biased guiding electrode further increased the number of protons reaching the target. These results demonstrate the effectiveness of the Negative Target concept for enhancing proton transport.

Keywords: pyroelectric fusion, proton-boron fusion, beam current, elementary processes, numerical analyses

DOI: 10.1585/pfr.21.1205048

Pyroelectric crystals generate high electric potentials through temperature-induced variations in their polarization state, making them attractive for compact particle accelerator applications. Commercial pyroelectric X-ray sources are already used in analytical techniques such as X-ray absorption spectroscopy and X-ray fluorescence analysis [1]. Naranjo *et al.* first demonstrated deuterium-deuterium (D-D) fusion using a lithium tantalate ($LiTaO_3$) crystal and an erbium deuteride (ErD_2) target [2]. Since then, pyroelectric fusion has been investigated as a compact neutron source [3]. Among candidate fusion reactions, proton-boron (p-^{11}B) fusion has attracted attention because of its aneutronic nature and favorable fuel-handling characteristics. However, its fusion cross-section is only about 1.4 barns (10^{-28} m^2) at 675 keV [4], significantly smaller than that of deuterium-tritium (D-T) fusion, making ignition more challenging. Therefore, understanding the reaction environment and identifying conditions that enhance the fusion yield are essential for the development of p-^{11}B fusion systems. In this context, compact experimental platforms are valuable for investigating the underlying and evaluating physics. Pyroelectric crystal-based accelerators provide a promising approach because of their simple and compact configuration. In our previous studies, the effects of electrode configuration and temperature variation on the proton impact ratio were evaluated to identify optimal acceleration conditions [5, 6]. Although effective electrode configurations were identified, the proton-generation mechanism and proton transport behavior remain insufficiently understood. In this study, we further investigate these processes and explore conditions for enhancing the proton impact ratio.

In the present study, a new concept, termed the Negative Target (N Target), was introduced, in which protons are accelerated by a negative potential rather than the positive potential used in conventional configurations. The configuration was evaluated through numerical simulations, and its geometry is shown in Fig. 1.

Figure 1(a) shows the electrode configurations considered in this study. The figure represents a cross-sectional view in the *x*–*z* plane and all dimensions are expressed in meters (m). In the positive Disk Electrode configuration, the yellow region denotes the pyroelectric crystal, the black region represents the target, and the gray regions correspond to the electrodes. The electrodes located near the target are assigned to a separate potential structure, as described below.

Corresponding author's e-mail: t-tak@gunma-u.ac.jp

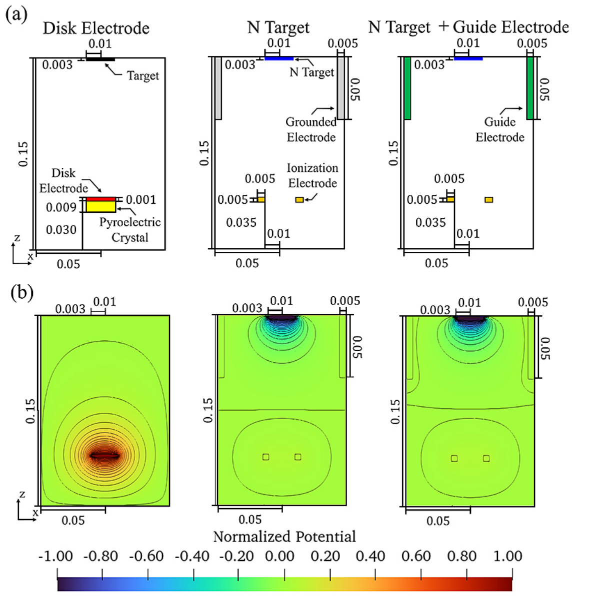

Fig. 1. (a) Schematic *x–z* cross sections of the experimental setup, showing three different electrode configurations (left [5, 6], center, and right panels). (b) Normalized potential distributions for the electrode configurations considered in this study. The dimensions indicated in the figure are given in meters (m).

In the Negative Target configuration shown in the center of Fig. 1(a), the target is assigned a negative potential originating from the pyroelectric crystal in order to accelerate protons. In this configuration, the crystal itself is assumed to be located outside the computational domain. The orange region at the center represents the ionization electrode. Electrons are trapped by the positive potential applied to this electrode and subsequently utilized for the proton-generation process described later. The configuration shown on the right-hand side of Fig. 1(a) further incorporates guiding electrodes designed to direct protons toward the target. In this case, the electrodes near the target are assigned potentials according to this guiding-electrode configuration. In Fig. 1(a), red and associated with the pyroelectric crystal, respectively. The ionization electrode (orange) is assigned a positive potential equal to 5% of the maximum negative potential to trap electrons and promote ionization, while the proton-guiding electrode (green) is assigned 0.5% to direct protons toward the target. The potential distribution inside the device was obtained by solving Laplace's equation. The maximum positive and negative potentials used as boundary conditions were derived from the integral form of Gauss's law following the methodology adopted in a previous study [5, 6]. The device wall was treated as a grounded boundary in the potential calculation. Since the magnitude of the generated potential depends on the crystal temperature change, temperature variations ranging from 0.1 to 100 K were considered in the present study. To describe the proton-generation process, ionization reactions involving hydrogen molecules were incorporated into the simulation. The eight reactions listed below were implemented, allowing the system to evolve from an initial electron-only state into a plasma consisting of multiple charged species.

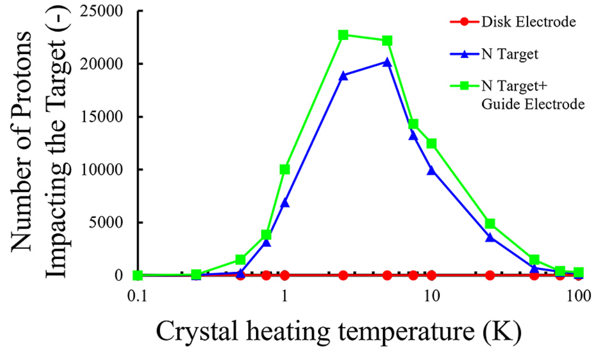

Fig. 2. Comparison of the number of protons impacting the target for different electrode and target configurations.

$$e^- + H_2 \rightarrow \begin{cases} 2e^- + H_2^+ \\ 2e^- + H + p \\ 3e^- + 2p, \end{cases} \tag{1}$$

$$H_2^+ + H_2 \rightarrow \begin{cases} H_2^{+*} + H_2 \\ H_2^* + H_2^+ \\ p + H + H_2 \\ H_3^+ + H \\ 2e^- + 2H_2^+ . \end{cases} \tag{2}$$

Equations (1) and (2) describe the reactions between an electron and a hydrogen molecule, and between a molecular hydrogen ion and a hydrogen molecule, respectively. In these equations, the asterisk (*) indicates an energetic species carrying the majority of the kinetic energy released in the reaction. As an initial condition, electrons were uniformly distributed throughout the device, excluding regions occupied by the electrodes and the target. During the trajectory calculation of each electron, the probability of each ionization reaction was determined from the corresponding reaction cross section as a function of particle energy [7–9], and the occurrence of reactions was evaluated using a Monte Carlo procedure based on random numbers. The same trajectory tracking and reaction evaluation were subsequently applied to newly generated charged particles. The simulation was continued until either 2 μs of physical time had elapsed or all charged particles had been lost from the system. The number of protons impacting the target was then counted to evaluate the proton impact characteristics.

Figure 2 presents the calculated numbers of protons impacting the target for the positive-electrode and Negative Target configurations. In addition, Fig. 1(b) shows the normalized potential distribution obtained from the calculation, with the equipotential contours superimposed. The geometrical dimensions are the same as those shown in Fig. 1(a). In the conventional positive Disk Electrode configuration, no protons reached the target because all charged particles stopped before 2 μs of physical time had elapsed. In contrast, the Negative Target configuration achieved the highest proton impact count at crystal temperature changes of 2.5–5 K, which was further enhanced by the application of a guiding-electrode potential. These results demonstrate the superiority of the Negative Target configuration for increasing proton impacts on the target.

This work was performed with the support and under the auspices of the NIFS Collaboration Research program (NIFS26KIPC004 and NIFS26KISC037).

[1] J. Kawai *et al.*, X-Ray Spectrom. **41**, 216 (2012).
[2] B. Naranjo *et al.*, Nature **434**, 1115 (2005).
[3] J. Geuther *et al.*, Phys. Rev. Lett. **96**, 054803 (2006).
[4] D. Gillich *et al.*, Nucl. Instrum. Methods Phys. Res. A **602**, 306 (2009).
[5] S. Inoue *et al.*, Plasma Fusion Res. **20**, 1205040 (2025).
[6] S. Inoue *et al.*, Plasma Fusion Res. **21**, 1405028 (2026).
[7] A.V. Phelps, J. Phys. Chem. Ref. Data. **19**, 653 (1990).
[8] R.K. Janev *et al.*, Collision Processes in Low-Temperature Hydrogen Plasmas (Forschungszentrum Jülich, 2003), 188.
[9] G.W. McClure, Phys. Rev. **130**, 1852 (1963).